

A Review: Magnetite Accelerated Corrosion of Secondary Side Materials in a PWR

Do Haeng Hur*, Geon Dong Song, Soon-Hyeok Jeon

Nuclear Materials Research Division, Korea Atomic Energy Research Institute,
989-111 Daedeok-daero, Yuseong-gu, Daejeon, 34057, Republic of Korea

*Corresponding author: dhhur@kaeri.re.kr

1. Introduction

Alloy 600 steam generator (SG) tubes are serviced in reducing and impurity-nearly free secondary water chemistry conditions [1]. Nevertheless, numerous Alloy 600 tubes have been affected by various corrosion related damages such as stress corrosion cracking (SCC), intergranular attack, and pitting. Destructive examinations for pulled tubes with corrosion defects from operating steam generators showed some evidences for high susceptibility to corrosion damages: Chemical impurities including chloride, sulfur-containing compounds, and lead etc. were detected inside the surface films and oxide-filled defects [2-4]. Acidic and alkaline chemistry deviated from the bulk water chemistry were also found to be a contributor [5-7]. These conditions could be induced preferentially in the heated crevices related with the top of tubesheet, tube support, and sludge pile, where harmful impurities can be concentrated by a local boiling process. The pH in the crevices is dependent on the species of anions and cations, their concentrations, and their molar ratio [8].

It should be noted that tubes and heated crevices in operating SGs are covered with deposits. The deposits are porous in nature and consist of mainly magnetite, of which origin is corrosion products released from carbon steel piping by flow accelerated corrosion. This means that real corrosion phenomena are occurring on the surface of a tube covered with porous magnetite. Therefore, the effects of magnetite deposit should be considered in evaluating the corrosion behavior of steam generator materials.

Therefore, the purpose of this paper is to review the extensive works being performed in our laboratory for the effects of magnetite deposit on the general corrosion of Ni-based alloys and carbon steel in various aqueous environments. The corrosion behaviors of Ni-based alloys and carbon steel will be reviewed separately.

2. Preparation of Magnetite Specimens

To evaluate the electrochemical corrosion behavior of magnetite itself, a compact and rigid magnetite working electrode is needed. Similarly, to evaluate the reaction mechanism at the interface between magnetite and metallic materials, a magnetite layer should be deposited on the localized area of the materials.

In our laboratory, various types of these magnetite deposited specimens were prepared by using the electrodeposition of the magnetite layer on a material matrix. The electrodeposition solutions consisted of 2 M

sodium hydroxide, 0.1 M triethanolamine, and 0.043 M ferric sulfate hydrate. The magnetite layer was electrodeposited in the deposition solution at an applied potential of $-1.05 V_{SCE}$ at $80^{\circ}C$. The detailed electrodeposition process of magnetite is given elsewhere [9, 10].

3. Ni-Based Alloys

Fig. 1 shows the potentiodynamic polarization curves of Alloy 690 and magnetite in the all volatile treated (AVT) solution with pH 9.5 at $60^{\circ}C$ [11]. The corrosion potential (E_{corr}) of magnetite was higher than that of Alloy 690. Therefore, when Alloy 690 and the magnetite are electrically contacted, Alloy 690 becomes the anodic element of the galvanic pair. Here, we can calculate the corrosion rate of Alloy 690 and magnetite at each E_{corr} using the Tafel extrapolation method. The galvanic corrosion rate can also be estimated by using the mixed potential theory. Therefore, if the two materials are coupled in equal area, the corrosion rate of coupled Alloy 690 will increase by about 2.6 times than that of non-coupled Alloy 690 due to the shift in its potential in the positive direction. Alloy 600 also revealed similar electrochemical behavior in the same test solution [12].

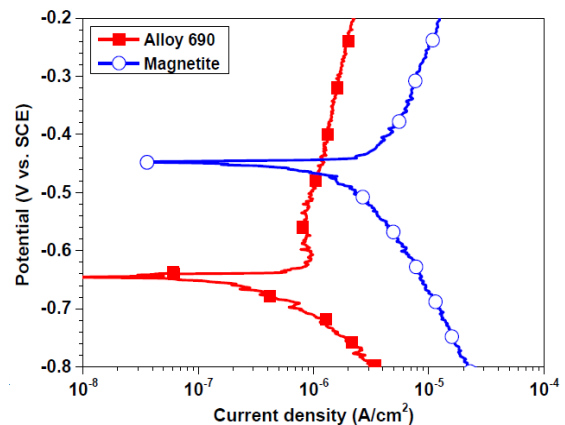


Fig. 1. Potentiodynamic polarization curves of Alloy 690 and electrodeposited magnetite in the AVT solution with pH 9.5 at $60^{\circ}C$.

Fig. 2 shows the polarization curves of Alloy 690 and magnetite in the AVT solutions with and without 1 M NaCl at $60^{\circ}C$ [13]. The E_{corr} of Alloy 690 was always lower than that of magnetite. This means that Alloy 690 behaves as an anode when Alloy 690 and magnetite are electrically connected. From these polarization curves,

we can calculate the corrosion rate (i_{corr}) of Alloy 690 and magnetite at each E_{corr} and at the mixed potential through the Tafel extrapolation method and mixed potential theory, respectively. The change of these corrosion rates are depicted in Fig. 3 [13]. Independently, the effect of chloride ions and galvanic coupling to magnetite produced a small effect on the corrosion rate of Alloy 690. However, the anodic dissolution rate of Alloy 690 was increased greatly by approximately 3.4 times when considering both the chloride ion effect and galvanic effect with magnetite.

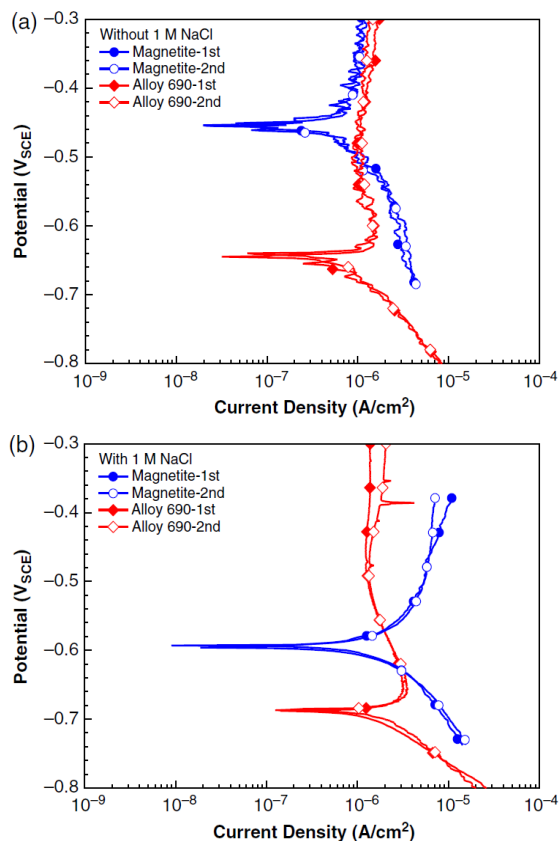


Fig. 2. Potentiodynamic polarization curves of Alloy 690 and magnetite in alkaline solutions of pH 9.5: (a) without and (b) with 1 M NaCl at 60°C.

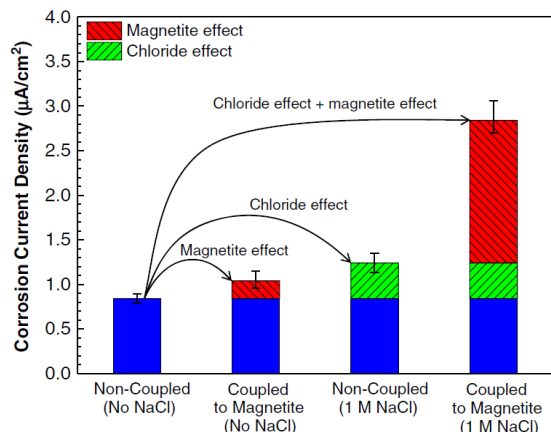


Fig. 3. Change in the anodic dissolution rate of Alloy 690 by the effects of chloride ions and magnetite in alkaline solutions of pH 9.5 at 60°C.

4. Carbon Steel

We examined the effect of magnetite on the corrosion of carbon steel in AVT solution [14] and polyacrylic acid (PAA)-containing AVT solutions [15]. The E_{corr} of magnetite was always higher than that of carbon steel in all test solutions. Thus, carbon steel acted as the anode of the galvanic couple between carbon steel and magnetite, resulting in an increased corrosion of carbon steel. Typically, Fig. 4 shows the polarization curves of carbon steel and magnetite in AVT solution of pH 9.5 with 100 ppm PAA at 25°C [15].

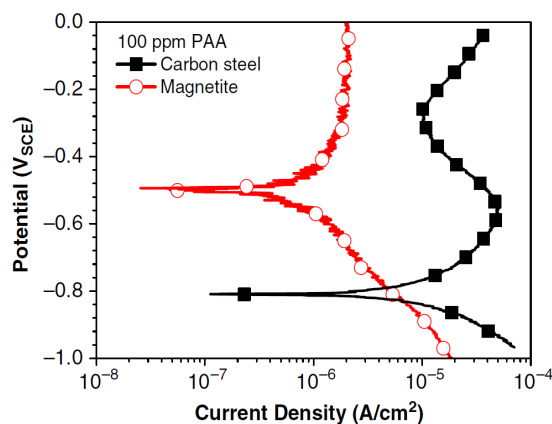


Fig. 4. Potentiodynamic polarization curves of carbon steel and magnetite in AVT solution of pH 9.5 with 100 ppm PAA at 25°C.

The effect of magnetite on the corrosion of carbon steel was also investigated in AVT water under flowing conditions at 60°C by using immersion and electrochemical tests [16]. From the immersion corrosion tests, it was clearly confirmed that the galvanic coupling with magnetite accelerated significantly the corrosion of carbon steel. In addition, the electrochemical behavior of carbon steel and magnetite showed that carbon steel acts as the anode of the galvanic couple with magnetite, resulting in an increased corrosion current. Therefore, the galvanic coupling of carbon steel with magnetite is proposed as an additional acceleration factor on the corrosion of carbon steel piping under severe turbulent flowing conditions in the secondary system of PWRs.

Fig. 5 schematically presents the electrochemical corrosion behavior in the regions where flow accelerated corrosion is most severe by a turbulent flow with a higher flow velocity [16]. The electrochemical behavior of carbon steel and magnetite demonstrated that the corrosion current of carbon steel was more increased by not only the mass transfer effect but also a galvanic corrosion mechanism. This galvanic corrosion mechanism was also supported by the results obtained from ZRA measurements. Thus, wall thinning of carbon steel piping will be more accelerated owing to the galvanic corrosion mechanism with magnetite under severe turbulent flowing conditions.

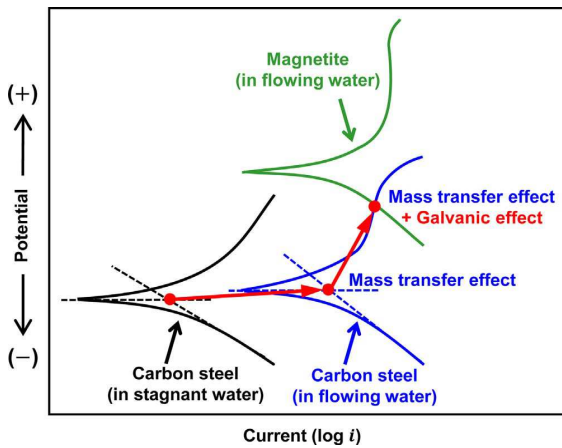


Fig. 5. Schematic of the electrochemical behaviors of carbon steel and magnetite occurring under a severe turbulent flow.

5. Conclusions

From this review of the effects of magnetite deposit on the general corrosion of Ni-based alloys and carbon steel, it is verified that magnetite coupled to the materials significantly accelerates the general corrosion rate of the materials in various aqueous environments. The galvanic coupling of carbon steel with magnetite is also proposed as an additional acceleration factor on the corrosion of carbon steel piping under severe turbulent flowing conditions in the secondary system of PWRs.

Actual corrosion phenomena are occurring in a condition where the surface of a SG tube is electrically contacted with porous magnetite deposits. Therefore, the effects of magnetite deposit should be considered in evaluating the corrosion behaviors of the secondary side materials in PWRs.

ACKNOWLEDGEMENT

This work was supported by the National Research Foundation of Korea (NRF) grant funded by the Korea government (2017M2A8A4015159).

REFERENCES

[1] EPRI, Pressurized Water Reactor Secondary Water Chemistry Guidelines - Revision 6, EPRI, Palo Alto, CA, USA (2004) 1008224.
[2] L. Thomas, B. Johnson, and S. Bruemmer, "Sulfur at crack tips in Alloy 600 service samples", Workshop of Effects of Pb and S on the Performance of Secondary Side Tubing of Steam Generators in PWRs, Argon National Laboratory, IL, May 24-27, 2005.
[3] King, F. Gonzalez and J. Brown, "Stress corrosion experience in steam generators at Bruce NGS", Proceedings of Sixth International Symposium on Environmental Degradation of Materials in Nuclear Power Systems - Water Reactors, San Diego, CA, TMS (1993) 233-240.
[4] D.H. Hur, M.S. Choi, D.H. Lee, M.H. Song, and J.H. Han, Pitting corrosion and its countermeasures for pressurized water reactor steam generator tubes, Corrosion 62 (2006) 905-910.

[5] D.H. Hur, M.S. Choi, D.H. Lee, M.H. Song, and J.H. Han, Root causes of intergranular attack in an operating nuclear steam generator tube, Journal of Nuclear Materials 375 (2008) 382-387.
[6] J.B. Boursier, M. Dupin, P. Sosset, Y. Rouillon, "Secondary side corrosion of French PWR steam generator tubing: Contribution of surface analyses to the understanding of the degradation process", Proceedings of Ninth International Symposium on Environmental Degradation of Materials in Nuclear Power Systems - Water Reactors, Newport Beach, CA, TMS (1999) 555-563.
[7] R.W. Staehle, and J.A. Gorman, Quantitative assessment of submodes of stress corrosion cracking on the secondary side of steam generator tubing in pressurized water reactors: Part 3, Corrosion 60 (2004) 115-180.
[8] EPRI, PWR Molar Ratio Control Application Guidelines, Volume 1, EPRI, Palo Alto, CA, USA (1995) TR-104811.
[9] C. Goujon, T. Pauporte, C. Mansour, S. Delaunay, and J-L. Bretelle, Electrochemical deposition of thick iron oxide films on nickel based superalloy substrates, Electrochimica Acta 176 (2015) 230-239.
[10] S.H. Jeon, G.D. Song, D.H. Hur, Effects of deposition potentials on the morphology and structure of iron-based films on carbon steel substrate in an alkaline solution, Advances in Materials Science and Engineering 2016 (2016) Article ID 9038478.
[11] S.H. Jeon, G.D. Song and D.H. Hur, Galvanic corrosion between Alloy 690 and magnetite in alkaline aqueous solutions, Metals, Vol.5, p. 2372-2382, 2015.
[12] S.H. Jeon, G.D. Song and D.H. Hur, Corrosion behavior of Alloy 600 coupled with electrodeposited magnetite in simulated secondary water of PWRs, Materials Transactions, Vol.56, p.2078-2083, 2015.
[13] G.D. Song, S.H. Jeon, J.G. Kim, D.H. Hur, Synergistic effect of chloride ions and magnetite on the corrosion of Alloy 690 in alkaline solutions, Corrosion, Vol.73, p.216-220, 2017.
[14] S.H. Jeon, G.D. Song and D.H. Hur, Electrodeposition of magnetite on carbon steel in Fe(III)-triethanolamine solution and its corrosion behavior, Materials Transactions, Vol.56, p.1107-1111, 2015.
[15] G.D. Song, S.H. Jeon, J.G. Kim, D.H. Hur, Effect of polyacrylic acid on the corrosion behavior of carbon steel and magnetite in alkaline aqueous solutions, Corrosion, Vol.72, p.1010-1020, 2016.
[16] G.D. Song, S.H. Jeon, Y.H. Son, J.G. Kim, D.H. Hur, Galvanic effect of magnetite on the corrosion behavior of carbon steel in deaerated alkaline solutions under flowing conditions, Corrosion Science, Vol.131, p.71-80, 2018.